Polymer Inhibitors Enable >900 cm^2 Dynamic Windows based on Reversible Metal Electrodeposition with high Solar Modulation

Michael T. Strand[1,2], Tyler S. Hernandez[2,3], Michael G. Danner[2], Andrew L. Yeang[2], Nathan Jarvey[2], Christopher J. Barile[4], Michael D. McGehee[2,5,6*]

1. Department of Materials Science and Engineering, Stanford University, Stanford, CA 94305, USA
2. Department of Chemical and Biological Engineering, University of Colorado, Boulder, CO 80303, USA
3. Department of Chemistry, Stanford University, Stanford, CA 94305, USA
4. Department of Chemistry, University of Nevada, Reno, Reno, NV 89557, USA
5. National Renewable Energy Laboratory, Golden, CO 80401, USA
6. Materials Science and Engineering, University of Colorado, Boulder, CO 80303, USA

*E-mail: michael.mcgehee@colorado.edu (ORCID: 0000-0001-9609-9030)

Abstract

Dynamic windows with adjustable tint give users control over the flow of light and heat to decrease the carbon footprint of buildings and improve the occupants' comfort. Despite the benefits of dynamic windows, they are rarely deployed in buildings because the existing technology cannot achieve fast and color-neutral tinting at an agreeable cost. Reversible metal electrodeposition (RME) is a promising approach to solve these problems. Here, we demonstrate the use of polymer inhibitors to reversibly deposit metal films with controlled morphology in dynamic windows. The windows that employ the polymer inhibitor can readily tint to below 0.001% visible transmittance in less than 3 minutes and exhibit high infrared reflectance (>70%), color-neutral transmittance ($C^* < 5$), and an ultrawide range of optical and solar modulation ($\Delta T_{vis} = 0.76$ and $\Delta SHGC = 0.56$). The polymer inhibitors also increase the efficiency and improve the durability of the windows and enable construction of >900 cm^2 dynamic windows with fast response and excellent uniformity.

Mastery over the flow of light and heat is an increasingly critical component of the global effort to combat climate change.[1] Passive technologies like low-emissivity coatings and radiative coolers can greatly reduce energy usage under certain conditions but lack the ability to adapt to dynamic (diurnal and seasonal) environments.[2–6] Dynamic windows with adjustable tint are an encouraging solution to simultaneously improve energy efficiency and human wellness.[7,8]

Dynamic windows yield an average 20% energy savings in buildings through reductions in lighting, heating, and cooling loads and are classified as a critical need for decarbonization of buildings.[9,10] Beyond energy savings, there is increasing evidence of the importance of natural light and office buildings with dynamic windows provide measured benefits to health, happiness, and productivity for their workers.[11,12] Despite the positive attributes of dynamic windows, market penetration is miniscule with current adoption in only 0.004% of commercial building space.[13]

Dynamic windows based on reversible metal electrodeposition (RME) are poised to overcome challenges with cost, color, contrast, and durability that have stalled adoption of traditional technologies based on electrochromic oxides and molecules.[14] Metals are robust materials with excellent photo-, thermal-, and chemical stability.[15] Further, the architecture of RME dynamic windows enables a wider range of visible and solar radiation control than any existing technology. Static metal coatings have been employed in windows for over forty years to manufacture windows that transmit visible light and reject heat.[16] *Dynamic* metal glazings introduce a paradigm where users (or algorithms) can control the visual and thermal properties of windows for optimal comfort and energy efficiency.

RME dynamic windows are electrochemical devices with two transparent electrodes that sandwich an electrolyte layer composed of colorless metal cations (Figure 1). The dynamic window operates on the electrochemical phase change between metal ions dissolved in the electrolyte and metal films that plate on the transparent electrodes and block light. The morphology of the metal film informs the critical optical properties like visible transmittance and solar heat gain.[17] Previous attempts to control the metal morphology focused on controlling the metal nucleation at the electrode surface.[18,19] Despite controlled nucleation, however, the metal films tend to be porous and inefficient at blocking light.[20]

In this article, we show that addition of polyvinyl alcohol (PVA) to a reversible plating solution yields smooth, compact metal films that are efficient at modulating light and heat flow. Dynamic windows that employ the polymer additive can readily tint to below 0.001% visible transmittance in under 3 minutes and exhibit high IR reflectance (>70%), color-neutral transmittance ($C^* < 5$), and a wider range of visible and solar modulation than any existing technology. The improved optical and electrical properties of the metal films grown with PVA allow for construction of >900 cm^2 dynamic windows with fast and uniform tinting. Lastly, the polymer additive advances the durability of RME dynamic windows by promoting stable and reversible electrodeposition over thousands of cycles.

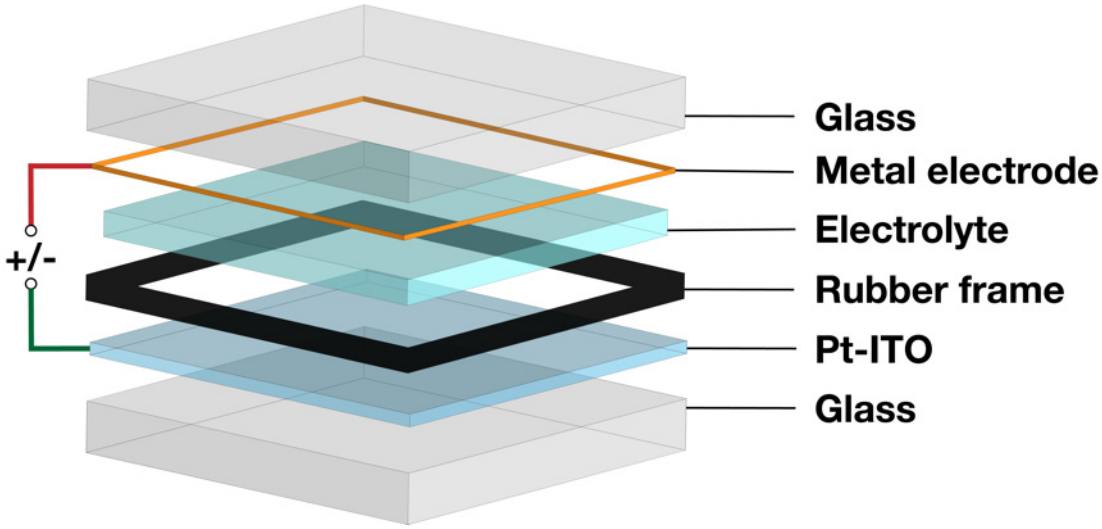

Figure 1. Schematic of Dynamic Window based on Reversible Metal Electrodeposition. The electrolyte is framed by a butyl rubber edge seal and sandwiched between a platinized indium tin oxide (Pt-ITO) electrode and metal frame electrode. Each electrode is adhered to a glass support. Applying a cathodic (reducing) potential between the Pt-ITO and metal electrode induces metal plating (i.e. tinting) and an anodic (oxidizing) potential causes the metal to dissolve back into the electrolyte (i.e. bleaching). The opposite (counter) reactions occur on the metal electrode to complete the circuit.

Polymer Inhibitors Promote Smooth Metal Growth

In RME dynamic windows, it is desirable to grow smooth and compact metal films that are efficient at modulating light. Polymer inhibitors promote this morphology by inducing a uniform plating rate at the surface and suppressing dendritic growth through an adsorption mechanism.[21] Without the inhibitor, localized electric fields form at inhomogeneities and yield dendritic electrodeposition (Figure 2A).[22] With the adsorbed polymer, however, the space charge remains distributed rather than localized over the surface and electrodeposition occurs uniformly (Figure 2B-C). Polyols, in particular, are promising inhibitors for dynamic windows because they are colorless, non-toxic, cheap, electrochemically stable, and compatible with reversible electrodeposition chemistry.[23,24]

We investigated whether polyvinyl alcohol (PVA) is a suitable inhibitor for dynamic windows by adding it to a reversible metal electrolyte and characterizing the electrodeposit morphology. The aqueous electrolyte employs Cu^{2+} and Bi^{3+} as the active metal ions because these metals share a similar standard reduction potential (+0.337 V and +0.308 V, respectively) and exhibit synergy during electrodeposition that improves reversibility.[25] The transparent electrodes where the metal plating occurs consist of indium tin oxide (ITO) on glass that is decorated with a sub-monolayer of 3-nm-diameter Pt nanoparticles to promote uniform nucleation of the metal electrodeposits.[19] We refer to the electrodes as Pt-ITO herein. In Figure 2D-G, we present SEM and AFM measurements for Bi and Cu metals deposited at -0.8 V vs. Ag/AgCl for one minute on Pt-ITO with and without a 0.1 wt.% addition of PVA (M_w: 61,000) to the electrolyte. The control film grown without any additives (i.e. 0% PVA) is rough (RMS: 46.2 nm) and

comprised of metal pillars with a wide size distribution and low surface coverage (Figure 2D-E). The plating solution with 0.1 wt.% PVA, in contrast, deposits a smooth (RMS: 4.05 nm), uniform morphology (Figure 2F-G). The metal film is compact and comprised of particles with a relatively narrow size distribution.

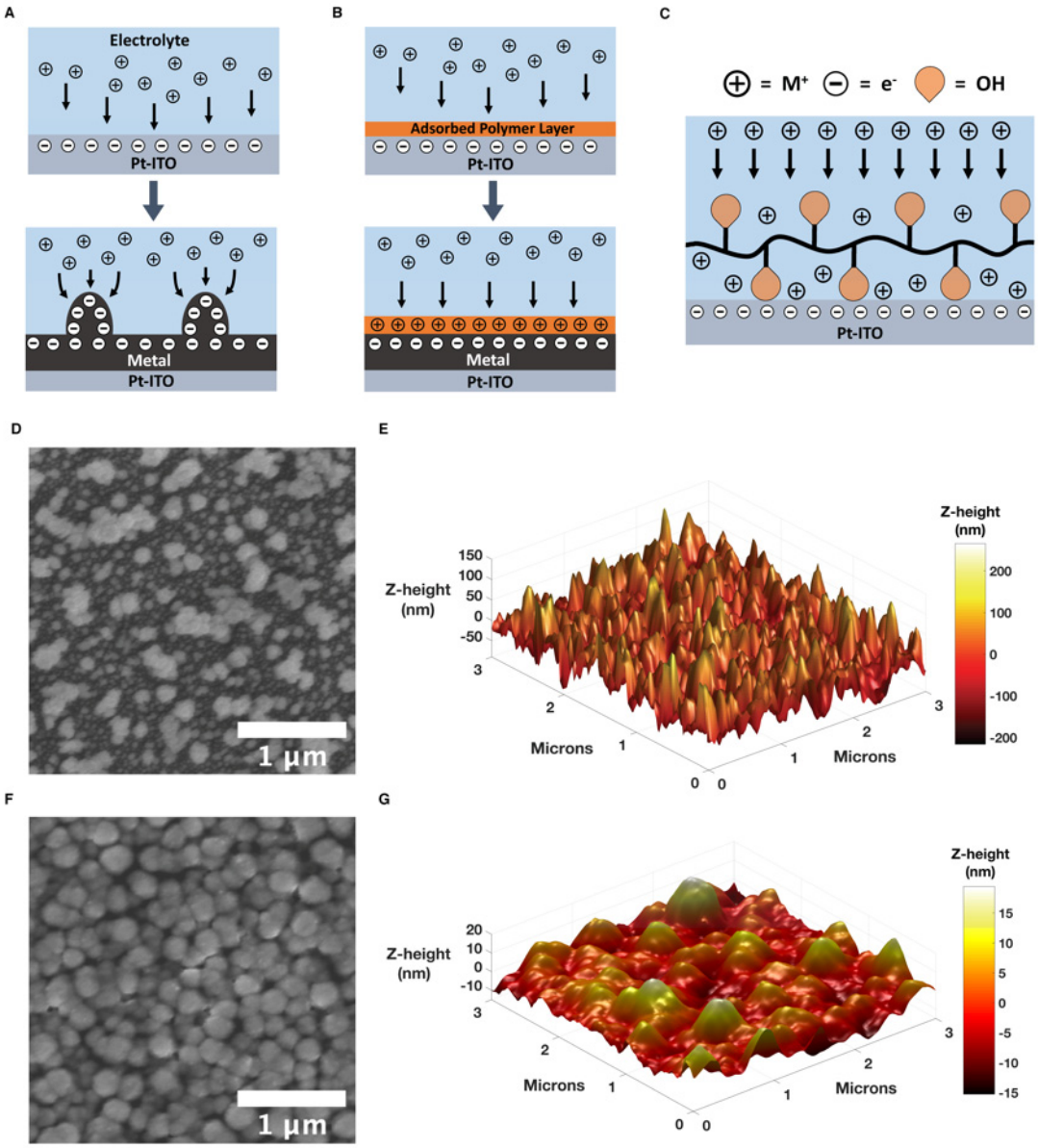

Figure 2. Morphology Control with Polymer Inhibitor. A) Schematic illustration of dendritic metal electrodeposition that occurs without electrolyte additives. B) Schematic illustration of how adsorbed polymer inhibitors promote smooth metal electrodeposition. The arrows between the panels indicate the direction of time as metal deposition occurs. C) Magnified view of electrode-electrolyte interface with adsorbed polyol inhibitor. The polymer adsorbs to the electrode and homogenizes the flux of metal cations to the plating surface. D) SEM of metal electrodeposits after 1 minute of deposition without electrolyte additives. E) AFM of electrodeposits presented in Figure 1D). F) SEM of metal electrodeposits after 1 minute of deposition with 0.1 wt.% PVA dissolved in the plating solution. G) AFM of electrodeposits presented in Figure 1F). Note scale bar difference in 1E,G. For the samples measured in Figure 1D-G, -0.8 V versus Ag/AgCl was applied to Pt-ITO electrodes.

The evolution of the film morphology shown in Figure 2D-G is presented in Supplementary Figures 1-2 as a series of tilted-view and top-down SEM images at different deposition times. The metal film composition is 43.6% Bi and 56.4% Cu (by atomic percentage) as measured with energy-dispersive X-ray spectroscopy (EDS) and is unaffected by the PVA as shown in Supplementary Table 1. Please refer to Supplementary Notes 1-3 for detailed electrochemical characterization of the polymer inhibitors studied in the work.

Superior Optical Performance

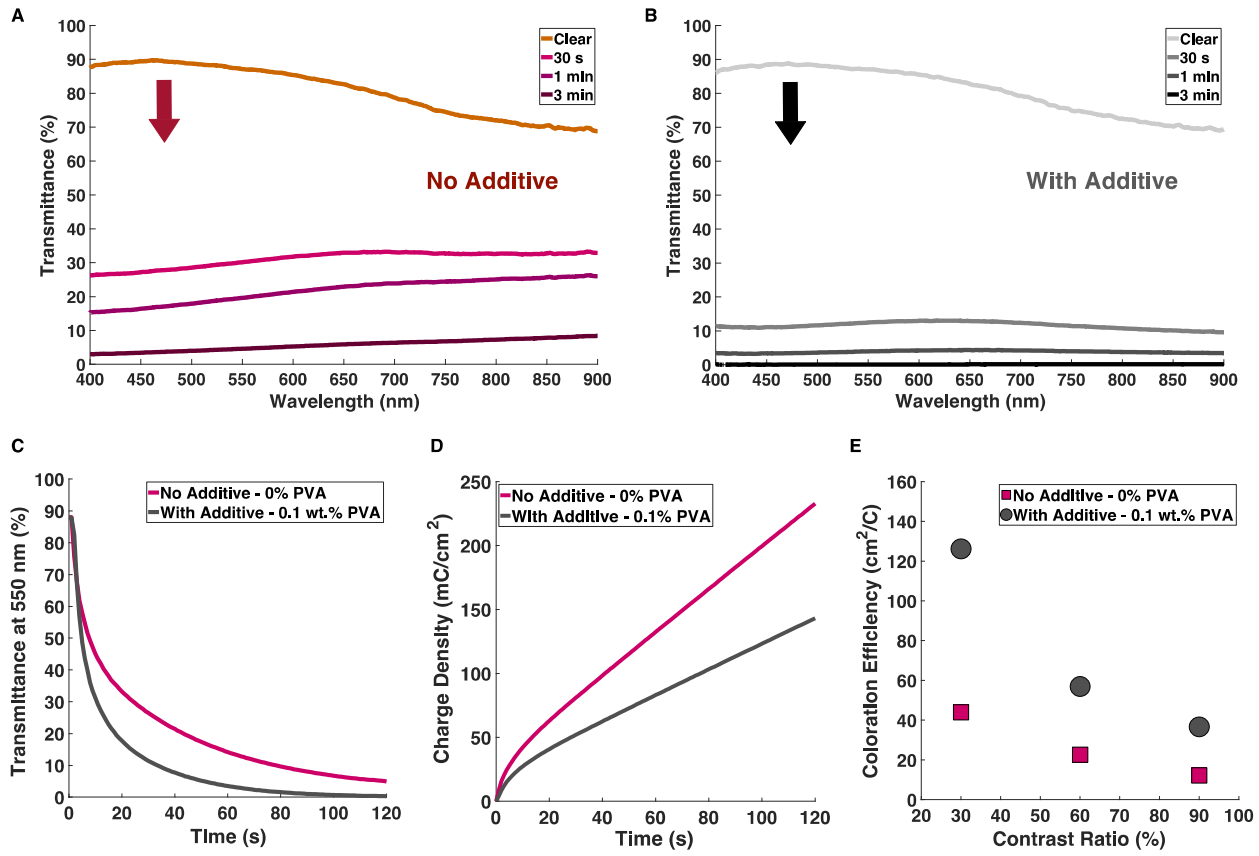

Figure 3. Optical Efficiency of Dynamic Windows. Transmittance spectra of A) 5 cm x 5 cm dynamic window without additive and B) 5 cm x 5 cm dynamic window with 0.1 wt.% PVA after four different deposition times. The vertical arrows indicate the direction of transmittance change as the window tints. C) Transmittance at 550 nm (where the human eye is most sensitive) versus time for 120 seconds of metal deposition and D) the charge density versus time required for the deposition. E) Coloration efficiency at 550 nm versus contrast ratio calculated with data in Figure 2C-D. A plating voltage of -0.8 V was applied to the dynamic window for three minutes to elicit metal deposition.

To measure the optical properties of the different metal morphologies, we fabricated 5 cm x 5 cm dynamic windows with and without the polymer inhibitor in the electrolyte and performed in-situ transmittance measurements during three minutes of tinting at a potential of -0.8 V. The transmittance spectra at four different time points are plotted for the control device (without additives) in Figure 3A and

for the dynamic window with 0.1 wt.% PVA in the electrolyte in Figure 3B. A schematic view of the dynamic window architecture is presented in Figure 1 and photographs of the devices are shown in Supplementary Figure 3. The transmittance at 550 nm versus switching time is plotted for both devices in Figure 3C. By comparing the optical response of the control device (without additives) and the dynamic window that contains 0.1 wt.% addition of PVA in the electrolyte, it is clear that the dense metal morphology promoted by the PVA elicits improved switching speed, neutral color (i.e. flat response across the visible spectrum), and contrast (down to 0.001% transmittance for privacy).

The polymer inhibitor also makes the dynamic windows more efficient. Coloration efficiency is an important metric for assessing dynamic windows and is defined as the change in optical density over a fixed area per unit charge. Dynamic windows with higher coloration efficiency require less energy to switch and yield less voltage drop across practical-scale electrodes.[19] In Figure 3D, we plot the charge density versus time and show that the rate of charge consumption is lower for the dynamic window with the PVA inhibitor. The combination of the lower rate of charge consumption and the increased switching speed (Figure 3C-D) gives the dynamic window with the polymer inhibitor a coloration efficiency that is 2-3x higher than the control device depending on the desired contrast (Figure 3E).

The improvement in optical performance and efficiency is attributed to the metal film morphology that forms in the presence of PVA. Without any additives in solution, the metal film is discontinuous and light can transmit through the gaps between metal deposits (Figure 2D-E, Supplementary Figure 1). The 'spiky' particles also increase scattering and yield a film that is absorptive, and thus poor at rejecting heat (Supplementary Figure 4A). The polymer inhibitor slows down the plating rate and supports deposition of a smooth and dense metal morphology (Figure 2F-G, Supplementary Figure 2). This film morphology yields windows that are more reflective (and less absorptive), especially in the NIR wavelengths that we experience as heat (Supplementary Figure 4B). The use of polymer inhibitors for controlling the electrodeposit morphology is important for achieving an energy-efficient optical response in terms of both power consumption and heat rejection in dynamic windows.

We further investigated the optical performance of dynamic windows with PVA by measuring the transmittance (T) and reflectance (R) in the $300 < \lambda < 2500$ nm wavelength range corresponding to solar radiation over the series of optical states accessible to the technology. $T(\lambda)$ and $R(\lambda)$ are plotted in Figure 4A-C for seven distinct optical states of dynamic windows with the PVA inhibitor. The shape of the transmittance spectrum in the clear state is determined by the transmittance through the ITO and aqueous electrolyte along with the two outer layers of glass. This shape is maintained as the window tints because the electroplated metal film blocks light uniformly across the solar spectrum. An important advantage of metal-based dynamic windows over competing technologies is an exclusive 'privacy state' with 0.001% visible transmittance that functions like blackout curtains for providing quality sleep (Figure 4A).[26] The privacy state is made possible by the dense metal morphology facilitated by the PVA inhibitor.

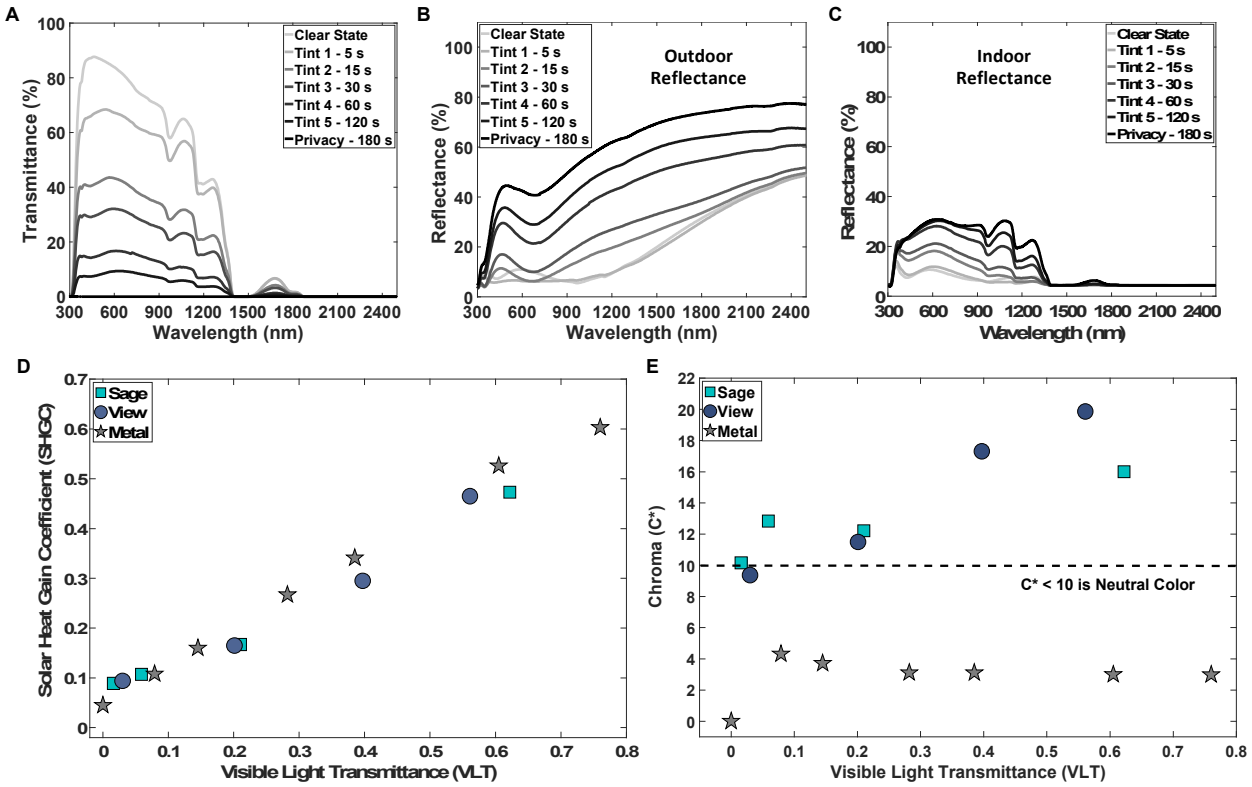

Figure 4. Optical Performance of Metal-Based Dynamic Window and its Comparison to Commercial Dynamic Windows. A) Transmittance spectra of metal-based dynamic windows for seven distinct optical states and the switching times required to achieve each state. B) Reflectance spectra measured through the ITO-on-glass electrode where the metal film initially forms for the seven optical states (outdoor reflectance). C) Reflectance spectra measured through the metal counter electrode that samples the top surface of the deposited metal films (indoor reflectance). D) Solar heat gain coefficient (SHGC) versus visible light transmittance (VLT) for the optical range of metal-based dynamic windows (Metal) compared to industry leaders Sage Glass (Sage) and View, Inc. (View). The grey shaded region indicates the dynamic range of the metal-based dynamic window and the blue shaded region indicates the dynamic range of the commercial dynamic windows. E) Chroma (C^*) versus visible light transmittance (VLT) with the condition for neutral color indicated. All optical data for the Sage and View windows were obtained from a public database (IGDB v29.0).

The reflectance spectrum in the clear state is primarily dictated by the ITO that serves as a low-emissivity coating that transmits visible light and reflects infrared wavelengths ($\lambda > 1200$ nm). The reflectance increases across the solar spectrum as the window tints because the metal film becomes more reflective as it grows. The high infrared reflectance ($700 < \lambda < 2500$ nm) of up to 70% is important for energy control as 1/2 of solar energy is in this regime. Additionally, the reflectance properties of the dynamic windows differ with the viewing direction (Figure 4B vs. Figure 4C). The reflectance spectra in Figure 4B were measured through the side of the device with the ITO electrode, and the spectra in Figure 4C were measured through the side of the device with the metal counter electrode. The surface where the metal nucleates (i.e. the ITO electrode) is more reflective while the top surface of the metal (shown in Figure 2F-G) is more absorptive. Further, light that reflects off the top surface of the metal must travel back through the electrolyte where it can be scattered or absorbed. Thus, the reflective surface can be oriented towards the exterior of the building where it can efficiently reject light and heat. The absorptive

side can face inward where a mirror-like appearance may be aesthetically undesirable to the people indoors. The dynamic windows also exhibit excellent bi-stability and do not require any additional power to maintain an optical state.[14,20] In Supplementary Figure 5, we present optical monitoring of a dynamic window that maintains the privacy state for 35 hours at open-circuit as further evidence of the energy savings potential of this technology.

Haze is an important metric for windows that describes the optical clarity and is the percentage of transmitted visible light that is scattered. The diffuse transmittance and total transmittance spectra of the dynamic windows measured with an integrating sphere at three different optical states are presented in Supplementary Figure 6. There is virtually zero diffuse transmittance across the visible spectrum which explains the low measured haze values (Haze: 0.12% at T_{vis}: 82%, Haze: 0.91% at T_{vis}: 26%) and indicates the excellent optical clarity of the dynamic windows. The diffuse reflectance and specular reflectance spectra measured at three different optical states are presented in Supplementary Figure 7 and indicate the minimal light scattering off the dynamic windows.

The principal optical metrics for windows are the visible light transmittance (VLT) and the solar heat gain coefficient (SHGC). The VLT is the fraction of light in the visible spectrum ($400 < \lambda < 700$ nm) that passes through the window, weighted to the sensitivity of the human eye. A high VLT provides daylighting that can offset electric lighting, but also causes glare under direct sun. The SHGC is the percentage of solar radiation that enters a building through the window. This includes incident radiation that is directly transmitted through the window and absorbed radiation that is subsequently re-radiated into the building. A high SHGC is desirable in cold climates to offset heating loads, and a low SHGC is important in hot climates to manage cooling loads. Static windows use a spectrally-selective stack of metal films and anti-reflection layers with specific thicknesses that transmits visible light and reflects the near-infrared. The problem with static windows, however, is that the outdoor environment is in flux.

Dynamic windows that access a range of VLT|SHGC combinations introduce a new paradigm. With dynamic windows, users can adjust the optical properties according to the local climate without sacrificing the primary function of their window: the view. In our dynamic windows, with a modest voltage, the thickness of the metallic layer is adjusted to strike the right combination of daylighting and solar gain throughout each day. The best static windows use metal films to find this balance. The advance of *dynamic* metal films with tunable thickness could propel the next generation of windows that adapt to the user's preferences and environment.

To compare the optical performance of RME windows to other dynamic window technologies, we modelled a double-pane insulating glass unit (IGU) and calculated the performance metrics. A complete description and justification of the modelling parameters and calculations is provided in Supplementary Note 4. Figure 4D presents the VLT|SHGC space for metal-based dynamic windows ("Metal") and two commercially available dynamic window products from industry leaders View, Inc. and SageGlass based on specifications of the products published in the publicly available International

Glazing Database (IGDB v29.0). We plot VLT from Figure 4D on a logarithmic scale in Supplementary Figure 8 to emphasize the privacy state that is unique to windows that use metal electrodeposition. The "Metal" IGU boasts the largest dynamic range of the technologies with $\Delta T_{vis} = 0.76$ and $\Delta SHGC = 0.56$. The metal-based dynamic windows achieve a higher ΔT_{vis} than the competing technologies because the design does not require relatively thick (>1 μm) oxide electrodes that absorb visible light.[27,28] The dynamic windows achieve a superior $\Delta SHGC$ because of the high clear-state transmittance and reflective (versus absorptive) properties of the metal film (Figure 4B-C).

The color of windows is an equally important consideration. Most people prefer a neutral color transition (clear-to-gray-to-black) that does not distort the appearance of their indoor environment. Indeed, color is often cited as one of the largest drawbacks of existing technology that often appears yellow when clear and turns blue as it tints.[29] Chroma (C^*) is a measure of color in the CIE $L^*a^*b^*$ color space. When $C^* < 10$, the human eye has difficulty distinguishing the color of the object and it is perceived as gray (color-neutral). In Figure 4D, we plot the C^* vs. VLT for the three window technologies. The dynamic windows that use metal as the active layer exhibit neutral color over their entire optical range, unlike the competing technology. In Supplementary Figures 9-11, we plot projections of the $L^*a^*b^*$ coordinates for the optical states of each technology and convert the coordinates to RGB values to provide the reader with a visual understanding of the window colors.

>900 cm^2 Dynamic Windows

A major challenge for deploying electrochromic technologies at scale is minimizing voltage drop across the transparent electrode and achieving uniform tinting across the window. All materials (*sans* superconductors) possess internal resistance to current flow that scales with the distance the charge must traverse. For windows, this problem is exacerbated by the requirement for transparent conductors that are generally 100x more resistive than common conductors like copper.[30] We published an analytical model of electrode resistance for electrochromic windows and derived a simple equation for the voltage drop across a square electrode (equation 1).[19] The voltage drop often yields non-uniform tinting.

$$\Delta V = \frac{JR_{sh}L^2}{8};\ J = current\ density, R_{sh} = sheet\ resistance, L = electrode\ length \quad \text{(eq. 1)}$$

There are several strategies for achieving uniform tinting over large-area (> 1 m^2) windows. The most common approach is to slow down the switching speed and thus lower the current density required for the window to tint. As a result, the majority of commercial electrochromic windows take ~20 minutes to transition across their optical range.[31,32] Kinestral Technologies has pioneered the use of patterned electrodes that enable their Halio® product to tint "10x faster" than incumbent technologies, but this perk comes at a cost premium.[33] A final strategy to achieve fast and uniform tinting is to decrease the sheet resistance of the electrodes. However, none of the efforts to reduce the electrode resistance have been successful at a large scale.

Dynamic windows based on reversible metal electrodeposition (RME) enable a unique strategy for reducing the resistance of the electrodes. Metals are excellent conductors and deposition of continuous metal films decreases the resistance of the electrodes as the metal film grows thicker.[34] This approach was not possible in previous generations of RME windows, because the metal electrodeposits were isolated and discontinuous (Figure 2D-E). With the PVA inhibitor, the metal film has an uninterrupted morphology as shown in Figure 2F-G that yields increased electrode conductivity as the window tints.

In Figure 5, we characterize the electrical properties of the metal film as it grows on the Pt-ITO transparent electrode. Figure 5A plots the current density and charge density versus time for 300 seconds of electrodeposition at -0.8 V and Figure 5B shows the decrease in electrode sheet resistance as the metal film grows thicker over time. The corresponding voltage drop across a 929 cm^2 ITO electrode was calculated using Eq. 1 and plotted in Figure 5C using the current density (J) in Figure 5A and the sheet resistance (R_{sh}) in Figure 5B across five different deposition times (15s, 30s, 60s, 120s, and 300s). We demonstrated in previous work that the electrodeposition rate is voltage-independent over some voltage range inherent to the electrolyte chemistry because the metal growth is diffusion-limited.[19] The voltage tolerance (i.e. the voltage range where the electroplating rate is uniform) is 0.6 V for the electrolyte used in this work.[25] The condition for uniform tinting in this system is highlighted in Figure 5C with a dashed line. The decrease in voltage drop over time plotted in Figure 5C indicates that uniform tinting is possible in a >900 cm^2 dynamic window after ~30 s of electrodeposition. To validate this hypothesis, we constructed a 929 cm^2 dynamic window and measured the transmittance (at 550 nm) versus time at three different spots from the center of the window to the edge (Figure 5D). As expected, the window tinted faster at the edge (where the voltage is applied) for the first 30 seconds. However, with further electrodeposition, the optical modulation in the center caught up to the edge and the visible response of the entire window was uniform. Photographs of the 929 cm^2 window are shown in the clear state (Figure 5E) and the dark state (Figure 5F) after 10 minutes of tinting. The optical response of the windows measured in Figure 5 is slower than the dynamic windows measured in Figure 4 because we reduced the active ion concentration from 10 mM to 5 mM to lower the current density (Supplementary Figure 12). Diluting the ion concentration was not a viable option in previous iterations of our work because the metal morphology became more porous upon dilution. The PVA inhibitor solves this problem by promoting a compact morphology, irrespective of ion concentration in the electrolyte.

The uniform deposition in a >900 cm^2 dynamic window is the culmination of three advantages of the PVA inhibitor: 2x improvement in coloration efficiency, 2x ion concentration dilution to halve the current density, and the 30% reduction in sheet resistance from the continuous metal film. The 2x improvement in coloration efficiency means that ½ the current is needed to switch the window at a fixed speed. By halving the metal ion concentration from 10 mM to 5 mM, the window operates at half the current density, and thus half the voltage drop across the electrode. The 30% reduction in sheet resistance lowers the voltage drop by an additional 30% (please refer to Supplementary Note 5 for analysis of the

theoretical change in sheet resistance from electrodeposition of a metal film on the ITO electrode). The combination of these three factors yields a tolerable voltage drop (< 0.6 V) for uniform tinting in a >900 cm^2 dynamic window based on reversible metal electrodeposition.

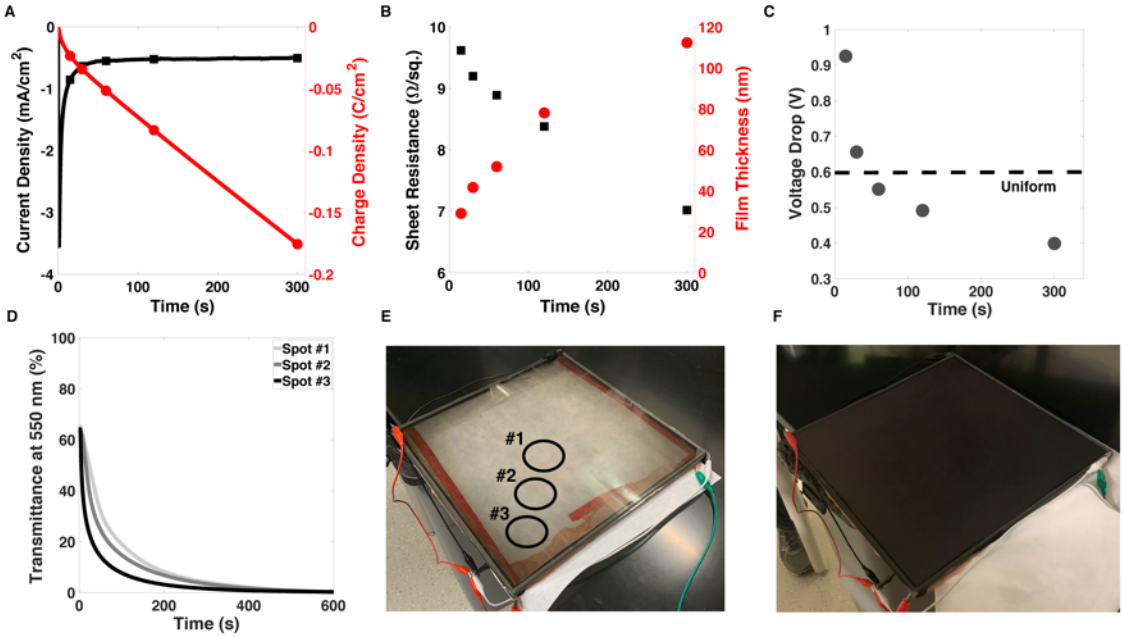

Figure 5. Uniform Tinting in >900 cm^2 Dynamic Window. A) Current density and charge density versus time for 300 seconds of electrodeposition. B) Sheet resistance and film thickness versus time for samples measured at five distinct deposition times (15s, 30s, 60s, 120s, 300s). C) Voltage drop from edge to center of a 929 cm^2 ITO electrode as a function of deposition time. D) Transmittance at 550 nm versus time measured at three different spots of a 929 cm^2 dynamic window to demonstrate uniform tinting from edge to center. E) 929 cm^2 dynamic window in clear state with uniformity measurement spots. F) 929 cm^2 dynamic window in dark state.

Durability

Long-term durability is a critical aspect of dynamic windows as conventional windows are expected to last in buildings for 20-30 years. Our previous work focused on improved durability through design of the electrolyte chemistry and yielded a formulation that demonstrated 10,000 tinting cycles with no observed degradation in a 3-electrode testing cell.[25] Of course, long-term durability must ultimately be proven using a complete device architecture for the technology to be commercially viable. In Figure 6A-C, we present optical and electrochemical data over 1,000 cycles for a 25 cm^2 dynamic window with 0.1 wt.% PVA in the electrolyte layer and with an identical device architecture to the 929 cm^2 window presented in Figure 5. We observe no degradation in switching speed or optical performance. We present cyclic voltammetry (CV) curves before and after 1,000 cycles in Supplementary Figure 13 and SEM of the electrodeposits after 1,000 cycles in Supplementary Figure 14. We observe no change in the CV curve or the electrodeposit morphology after 1,000 cycles. In previous iterations of our dynamic windows, the cycle life was limited by the durability of the copper mesh counter electrode that would fail after a few

hundred cycles.[19,25] The PVA inhibitor drastically improves the durability of the copper mesh by promoting uniform plating on the mesh and limiting the side reactions that degrade the mesh over cycling. In Figure 6D-E, we present microscope images of the copper mesh after 1,000 cycles with and without the polymer inhibitor as testament to the improved durability of the dynamic windows presented in this work. The mesh electrode in the device that contains 0.1% PVA in the electrolyte shows no signs of degradation after 1,000 cycles. We further analyze the performance of the window with PVA over 5,000 cycles in Supplementary Figure 15 and observe a slight decrease in switching speed under consistent cycling conditions. All of the durability testing in this work was performed at room temperature without solar exposure.

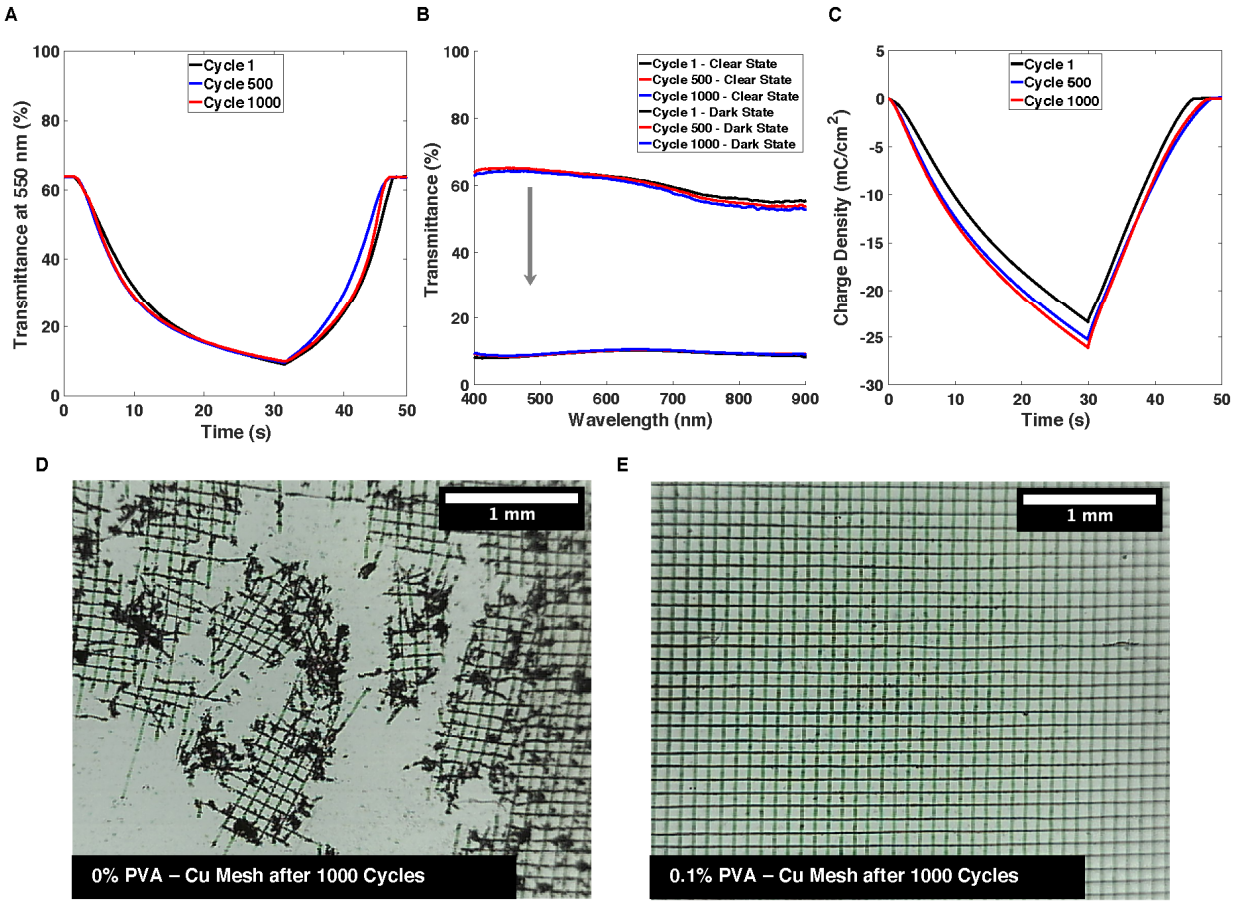

Figure 6. Durability of Dynamic Windows over 1000 Cycles. A) Transmittance at 550 nm versus time for Cycle 1, Cycle 500, and Cycle 1000. B) Transmittance spectra in clear state and dark state (-0.7 V for 30 s) for Cycle 1, Cycle 500, and Cycle 1000. The arrow indicates the direction of transmittance change during tinting from the clear state to the dark state. C) Charge density versus time for Cycle 1, Cycle 500, and Cycle 1000. Microscope images of Cu mesh counter electrode after 1000 cycles in D) device without PVA and E) device with 0.1 wt.% PVA added to the electrolyte. Cycling conditions: -0.7 V for 30 s, +0.7 for 30 s. All data in Figure 5A-C was obtained from cycling a 5 cm x 5 cm dynamic window with 0.1 wt.% PVA in the electrolyte layer and with an identical device architecture to the 929 cm^2 window presented in Figure 5.

Discussion

There are several remaining challenges before the widespread adoption of dynamic windows based on reversible metal electrodeposition. The durability standard for dynamic windows (ASTM 2141-14) stipulates 50,000 cycles over 5,000 hours under accelerated testing conditions (1-sun, 85 °C) with minimal degradation to prove the 20-30 year expected lifetime for the technology. We have future work aimed at passing this standard and understanding how the stressors effect the window performance over time. Kinestral Technologies has recently passed this durability test using a polymer electrolyte and has proven that long-term durability is attainable in dynamic windows that incorporate polymers.[35] It is also worth noting that polymers have been used in laminated glazings and windows for decades with excellent durability results.[36]

The >900 cm^2 dynamic windows presented in this work demonstrate an ultrawide dynamic range across the entire solar spectrum that is competitive with the state-of-the-art performance of traditional electrochromic materials.[37–40] We have outlined several strategies for maintaining fast switching speeds and uniform tinting as we continue to scale up towards meter-squared windows. We believe the unique advantages of reversible metal electrodeposition (along with the conventional strategies outlined earlier in the text) provide a clear path towards demonstration of meter-squared dynamic windows that tint uniformly across the entire dynamic range in under five minutes.

Finally, one of the largest barriers to adoption of dynamic window technologies is the cost and complexity of the sputtering facilities used to deposit thick, multilayer coatings on large panes of glass. Our metal-based dynamic window technology does not require sputtering of thick coatings and can be processed on polymer films to reduce the capital expense for manufacturing and enable retrofits.[28] The superior optical performance, reduced complexity and expense, and proven scalability of the dynamic windows based on reversible metal electrodeposition make this technology an excellent candidate for providing the energy-efficient windows of the future.

In this article, we demonstrate the use of polymer inhibitors for controlling the morphology and optical properties of metal films in dynamic windows based on reversible metal electrodeposition. By adding a low concentration of polyvinyl alcohol (PVA) to the electrolyte, we show reversible plating of smooth and compact metal films that improve the performance of the dynamic windows. The windows that employ the polymer inhibitor can readily tint to below 0.001% visible transmittance in less than 3 minutes and exhibit high infrared reflectance (>70%), color-neutral transmittance ($C^* < 5$), and an ultrawide range of optical and solar modulation ($\Delta T_{vis} = 0.76$ and $\Delta SHGC = 0.56$). The improved optical and electrical properties of the metal films grown with PVA allow for construction of >900 cm^2 dynamic windows with fast, uniform tinting and improved durability. The advances detailed in this manuscript are achieved with almost no additional complexity or expense and serve as testament to the commercial promise of dynamic windows based on reversible metal electrodeposition for saving energy in buildings.

Methods

Pt-ITO electrode preparation

ITO-on-glass transparent electrodes with a sheet resistance of 10 Ω/sq (Xinyan Technology Ltd.) were cleaned by ultrasonication in de-ionized H_2O with 10% Extran solution for 10 min, acetone for 5 min, and isopropanol for 10 min, sequentially. Next, the electrodes were dried under a stream of N_2 or air and then placed in a UVO-cleaner (Jelight Company Inc, Model No 42) for 10 mins to remove organic contaminants. To form the Pt-ITO electrodes, an aqueous dispersion of 1000 ppm Pt nanoparticles with 3 nm average diameter (Sigma-Aldrich) was diluted 10:1 with deionized water and then spray deposited with a 20 mm 113 kHz Ultrasonic Mist Atomizer (WHDTS) onto the ITO-on-glass electrodes. Then, the electrodes were annealed in air at 250°C for 20 minutes before use.

Electrochemical characterization

Electrochemical studies were carried out using a SP-150 Biologic potentiostat. For experiments utilizing three electrodes, electrochemical potentials were measured and reported in reference to a "no-leak" Ag/AgCl (3 M KCl) reference electrode (eDAQ). The immersed geometric surface area of the working electrode was 1.0 cm^2 for the three-electrode experiments. Spectroelectrochemical measurements were performed in a 4.5 cm by 2.0 cm by 1.0 cm glass cuvette (G205, Labomed, Inc.) in a three-electrode configuration with Pt-modified ITO-on-glass as the working electrode, a Pt wire counter electrode, and a "no-leak" Ag/AgCl (3 M KCl) reference electrode (eDAQ).

Electrolyte preparation

Chemicals were received from commercial sources and used without further purification. The perchlorate electrolyte comprised 10 mM $Cu(ClO_4)_2$, 10 mM $BiOClO_4$, 10 mM $HClO_4$, and 1 M $LiClO_4$ dissolved in deionized water. The halide-based electrolyte comprised 15 mM $CuCl_2$, 5 mM $BiCl_3$, 10 mM HCl, and 1 M LiBr dissolved in deionized water. The various polymer additives comprised polyvinyl(alcohol), polyethylene glycol, polyvinylpyrrolidone, and hydroxyethylcellulose. All the polymers were purchased from Sigma-Aldrich as powders and polymers with variable molecular weight were obtained for the relevant experiments. All polymers were dissolved in the control electrolyte by placing a vial of electrolyte with an immersed PTFE stir bar on a hot plate set to 60 C and 1200 RPM for 1 hour. The concentration of polymer in solution varied from 0.1 wt.% to 10 wt.% and was a variable of study.

5 cm x 5 cm dynamic window fabrication

Small-scale dynamic windows used for the optical performance characterization were constructed with 5cm x 5cm Pt-modified ITO on glass and a Cu foil frame around the edge (see Figure 1 for schematic). The electrolyte for the small-scale windows was the control electrolyte with 0.1 wt.% PVA (Mw = 61,000). Butyl rubber Solargain edge tape with a thickness of 2 mm and a width of 5 mm (Quanex Inc.) served as the frame of the dynamic windows. Conductive nylon tape (ElectricMosaic, Z22) enabled electrical contact to the perimeter of the ITO electrode. The total window thickness was 5 mm.

Large-area dynamic window fabrication

Large-area dynamic windows comprised the same layers as the 5 cm x 5 cm windows with the exception of the Cu mesh electrode used in place of the Cu foil frame. The windows were constructed with 30cm x 30cm Pt-modified ITO-on-glass or 5cm x 15cm Pt-modified ITO on glass and transparent Cu mesh (TWP, Inc., wire diameter: 0.0012 in) as the electrodes. The electrolyte for the prototypes had the same components as the control electrolyte with the concentration of the $Cu(ClO_4)$ and the $BiOClO_4$ diluted to 5 mM. Butyl rubber Solargain edge tape with a thickness of 2 mm and a width of 5 mm (Quanex Inc.) served as the frame of the dynamic windows. Conductive nylon tape (ElectricMosaic, Z22) enabled electrical contact to the perimeter of the ITO electrode.

Optical Characterization

In-situ optical measurements (transmittance and reflectance) were measured with an Ocean Optics FX spectrometer coupled with an Ocean Optics halogen light source (HL-2000-FHSA) and a reflectance probe. We do not have the capability to perform in-situ transmittance measurements of 1 $ft.^2$ devices but were able to perform the optical measurements on 6-inch dynamic windows with the electrode contact at one edge to simulate the behavior of a 1 $ft.^2$ window. Complete optical data used for the performance modeling was collected from 300-2500 nm with 2 nm increments using a Cary 5000 UV-VIS-NIR spectrometer coupled with a Universal Measurement Accessory (Cary, UMA).

Materials Characterization

SEM was performed with either a FEI NovaLab 600i scanning electron microscope operated at an accelerating voltage of 5 kV or an FEI Magellan 400 XHR scanning electron microscope operated at an accelerating voltage of 5 kV, or a JEOL JSM-7401F FESEM operated at an accelerating voltage of 5 kV and equipped with an EDS detector. Surface topology was measured with a NanoSurf easyScan 2 atomic force microscope.

Window Performance Modeling

Optical performance modeling was conducted using Window 7.7 (LBNL) and Optics 6 (LBNL) software. Glazing data for the View, Inc. and SageGlass windows was obtained from the International

Glazing Database (IGDB v29.0). Specifically, we used the Optics 6 software to analyze and convert the raw spectrophotometry measurements for the metal-based dynamic windows, and the WINDOW 7 software to model the IGU with the various glazing layers and degrees of tint. The WINDOW 7 software includes algorithms for calculating VLT and SHGC that are consistent with the standards set by ASHRAE SPC 142, ISO15099, and the National Fenestration Rating Council (NFRC). The dimensions of the IGU were selected to model a typical unit and the thickness and orientation of each layer is shown schematically in Supplementary Figure 35. The dynamic glass layer is 5 mm thick and faces outside of the building and the clear glass layer is 6 mm thick and serves as the inward-facing portion of the IGU. There is a 12.7 mm gas layer consisting of 90% Argon/10 % Air in between the glass layers. The NSG Pilkington Optifloat™ Clear glass product was selected as the clear glass layer because it has high visible and solar transmittance and neutral color.

Acknowledgements

This material is based upon work supported by the U.S. Department of Energy's Office of Energy Efficiency and Renewable Energy (EERE) under the Building Technologies Office Award Number DE-EE0008226 (M.D.M). Part of this work was performed at the Stanford Nano Shared Facilities (SNSF), supported by the National Science Foundation under award ECCS-1542152. This research was also supported by the COSINC-CHR administered by the College of Engineering and Applied Science at the University of Colorado – Boulder. T.S.H. and M.T.S. acknowledge the financial support of National Science Foundation Graduate Research Fellowships (No. NSF DGE-1656518). M.T.S. also acknowledges financial support of a Stanford Graduate Fellowship. A.L.Y acknowledges financial support of a Graduate Assistantship in Areas of National Need (GAANN) Fellowship from the Department of Education. The authors thank Lori Postak from Quanex for providing the Solargain edge tape used to fabricate the windows. The authors thank Dr. Tomoko Borsa at the University of Colorado for assistance with materials characterization.

Author Contributions

M.T.S, T.S.H, M.G.D, A.Y., N.J., and C.J.B. performed the experiments and analyzed the data. M.T.S, T.S.H, C.J.B, and M.D.M designed the experiments. M.T.S conceived the project. M.T.S and M.D.M wrote the manuscript. All authors discussed the results and commented on the manuscript.

Competing Interests

M.T.S, T.S.H, and M.D.M are co-founders of Tynt Technologies Inc., a company commercializing dynamic windows. All other authors declare no competing interests.

Data Availability

All the relevant data generated or analyzed in this study are included in the published article and the Supplementary Information file.

References

1. Burke, M., Hsiang, S. M. & Miguel, E. Global non-linear effect of temperature on economic production. *Nature* **527**, 235–239 (2015).
2. Hamberg, I. & Granqvist, C. G. Evaporated Sn-doped In2O3 films: Basic optical properties and applications to energy-efficient windows. *J. Appl. Phys.* **60**, R123–R160 (1986).
3. Jelle, B. P. *et al. Fenestration of today and tomorrow: A state-of-the-art review and future research opportunities*. *Solar Energy Materials and Solar Cells* **96**, 1–28 (North-Holland, 2012).
4. Mandal, J. *et al.* Hierarchically porous polymer coatings for highly efficient passive daytime radiative cooling. *Science (80-.).* **362**, 315–319 (2018).
5. Raman, A. P., Li, W. & Fan, S. Generating Light from Darkness. *Joule* **3**, 2679–2686 (2019).
6. Li, T. *et al.* A radiative cooling structural material. *Science* **364**, 760–763 (2019).
7. Lee, E. S., Yazdanian, M. & Selkowitz, S. E. The Energy-Savings Potential of Electrochromic Windows in the US Commercial Buildings Sector. *Lawrence Berkeley Natl. Lab.* (2004).
8. DeForest, N. *et al.* United States energy and CO2 savings potential from deployment of near-infrared electrochromic window glazings. *Build. Environ.* **89**, 107–117 (2015).
9. Sbar, N. L., Podbelski, L., Yang, H. M. & Pease, B. Electrochromic dynamic windows for office buildings. *Int. J. Sustain. Built Environ.* **1**, 125–139 (2012).
10. Building Technologies Office. R&D Roadmap for Emerging Window and Building Envelope Technologies. *United States Dep. Energy* 26–30 (2014).
11. Meister, J. C. The #1 Office Perk? Natural Light. *Harvard Business Review* (2018).
12. Hedge, A. & Nou, D. Effects of Electrochromic Glass on Computer Vision Syndrome. *Proc. Hum. Factors Ergon. Soc. Annu. Meet.* **62**, 378–382 (2018).
13. Dynamic Glass | Project Drawdown. Available at: https://www.drawdown.org/solutions/dynamic-glass. (Accessed: 4th March 2020)
14. Barile, C. J. C. J. *et al.* Dynamic Windows with Neutral Color, High Contrast, and Excellent Durability Using Reversible Metal Electrodeposition. *Joule* **1**, 133–145 (2017).
15. Callister, W.D., Rethwisch, D. G. Corrosion and Degradation of Materials. in *Fundamentals of Materials Science and Engineering* 690–720 (John Wiley, 2012).
16. Rissman, J. & Kennan, H. Low-Emissivity Windows. *American Energy Innovation Council* (2013). Available at: http://americanenergyinnovation.org/wp-content/uploads/2013/03/Case-Low-e-Windows.pdf. (Accessed: 5th March 2020)
17. Kelly, K. L., Coronado, E., Zhao, L. L. & Schatz, G. C. The Optical Properties of Metal Nanoparticles: The Influence of Size, Shape, and Dielectric Environment. *J. Phys. Chem. B* **107**, 668–677 (2003).
18. Araki, S., Nakamura, K., Kobayashi, K., Tsuboi, A. & Kobayashi, N. Electrochemical Optical-Modulation Device with Reversible Transformation Between Transparent, Mirror, and Black. *Adv. Mater.* **24**, OP122–OP126 (2012).
19. Strand, M. T. *et al.* Factors that Determine the Length Scale for Uniform Tinting in Dynamic Windows Based on Reversible Metal Electrodeposition. *ACS Energy Lett.* **3**, 2823–2828 (2018).
20. Hernandez, T. S. *et al.* Bistable Black Electrochromic Windows Based on the Reversible Metal Electrodeposition of Bi and Cu. *ACS Energy Lett.* **3**, 104–111 (2018).
21. Vereecken, P. M., Binstead, R. A., Deligianni, H. & Andricacos, P. C. The chemistry of additives in damascene copper plating. *IBM J. Res. Dev.* **49**, 3–18 (2005).
22. Chazalviel, J.-N. Electrochemical aspects of the generation of ramified metallic electrodeposits. *Phys. Rev. A* **42**, 15 (1990).
23. Hallensleben, M. L. Polyvinyl Compounds, Others. in *Ullmann's Encyclopedia of Industrial Chemistry* (Wiley-VCH Verlag GmbH & Co. KGaA, 2000). doi:10.1002/14356007.a21_743
24. Chen, L. *et al.* Electrochemical Stability Window of Polymeric Electrolytes. *Chem. Mater.* **31**, 4598–4604 (2019).
25. Hernandez, T. S. *et al.* Electrolyte for Improved Durability of Dynamic Windows Based on Reversible Metal Electrodeposition. *Joule* **4**, 1501–1513 (2020).
26. de Castella, T. The plague of light in our bedrooms. *BBC News* (2014).

27. Granqvist, C. G. Oxide electrochromics: An introduction to devices and materials. *Sol. Energy Mater. Sol. Cells* **99**, 1–13 (2012).
28. Islam, S. M., Hernandez, T. S., McGehee, M. D. & Barile, C. J. Hybrid dynamic windows using reversible metal electrodeposition and ion insertion. *Nat. Energy* **4**, 223–229 (2019).
29. Lo, C. K., Shen, D. E. & Reynolds, J. R. Fine-Tuning the Color Hue of π-Conjugated Black-to-Clear Electrochromic Random Copolymers. *Macromolecules* **52**, 6773–6779 (2019).
30. Gordon, R. G. Criteria for Choosing Transparent Conductors. *MRS Bull.* **25**, 52–57 (2000).
31. SageGlass Product Guide. Available at: https://www.sageglass.com/sites/default/files/productguide_mkt_48.pdf. (Accessed: 8th May 2020)
32. View, Inc. Product guide. Available at: https://view.com/sites/default/files/documents/product-guide.pdf. (Accessed: 8th May 2020)
33. Kinestral Technologies Inc. Halio ® Insulated Glass Unit (IGU). Available at: https://www.kinestral.com/resources/halio-insulated-glass-unit-igu/. (Accessed: 13th May 2020)
34. O'Connor, B., Haughn, C., An, K.-H., Pipe, K. P. & Shtein, M. Transparent and conductive electrodes based on unpatterned, thin metal films. *Appl. Phys. Lett.* **93**, 223304 (2008).
35. Kinestral's Halio Smart-Tinting Glass Becomes the Only Next-Generation Electrochromic Technology to Pass Rigorous ASTM E2141 Durability Testing. Available at: https://www.kinestral.com/kinestrals-halio-smart-tinting-glass-becomes-the-only-next-generation-electrochromic-technology-to-pass-rigorous-astm-e2141-durability-testing/. (Accessed: 29th November 2020)
36. Martín, M. *et al.* Polymeric interlayer materials for laminated glass: A review. *Construction and Building Materials* **230**, 116897 (2020).
37. Cai, G., Darmawan, P., Cheng, X. & Lee, P. S. Inkjet Printed Large Area Multifunctional Smart Windows. *Adv. Energy Mater.* **7**, (2017).
38. Cai, G. *et al.* Ultra-large optical modulation of electrochromic porous WO3 film and the local monitoring of redox activity. *Chem. Sci.* **7**, 1373–1382 (2016).
39. Cai, G. *et al.* Molecular Level Assembly for High-Performance Flexible Electrochromic Energy-Storage Devices. *ACS Energy Lett.* **5**, 1159–1166 (2020).
40. Li, X. H., Liu, C., Feng, S. P. & Fang, N. X. Broadband Light Management with Thermochromic Hydrogel Microparticles for Smart Windows. *Joule* **3**, 290–302 (2019).